12-1-2019

Multiphoton quantum-state engineering using conditional measurements

Omar S. Magaña-Loaiza
Louisiana State University

Roberto de J. León-Montiel
Universidad Nacional Autónoma de México

Armando Perez-Leija
Max Born Institute

Alfred B. U'Ren
Universidad Nacional Autónoma de México

Chenglong You
Louisiana State University

See next page for additional authors

Recommended Citation

Magaña-Loaiza, O., León-Montiel, R., Perez-Leija, A., U'Ren, A., You, C., Busch, K., Lita, A., Nam, S., Mirin, R., & Gerrits, T. (2019). Multiphoton quantum-state engineering using conditional measurements. *npj Quantum Information, 5* (1) https://doi.org/10.1038/s41534-019-0195-2

npj | Quantum Information

www.nature.com/npjqi

ARTICLE OPEN

Multiphoton quantum-state engineering using conditional measurements

Omar S. Magaña-Loaiza[1,2*], Roberto de J. León-Montiel[3], Armando Perez-Leija[4,5], Alfred B. U'Ren[3], Chenglong You[1], Kurt Busch[4,5], Adriana E. Lita[2], Sae Woo Nam[2], Richard P. Mirin[2] and Thomas Gerrits[2]

The quantum theory of electromagnetic radiation predicts characteristic statistical fluctuations for light sources as diverse as sunlight, laser radiation, and molecule fluorescence. Indeed, these underlying statistical fluctuations of light are associated with the fundamental physical processes behind their generation. In this contribution, we experimentally demonstrate that the manipulation of the quantum electromagnetic fluctuations of two-mode squeezed vacuum states leads to a family of quantum-correlated multiphoton states with tunable mean photon numbers and degree of correlation. Our technique relies on the use of conditional measurements to engineer the excitation mode of the field through the simultaneous subtraction of photons from two-mode squeezed vacuum states. The experimental generation of nonclassical multiphoton states by means of photon subtraction unveils novel mechanisms to control fundamental properties of light. As a remarkable example, we demonstrate the engineering of a quantum state of light with up to ten photons, exhibiting nearly Poissonian photon statistics, that constitutes an important step towards the generation of entangled lasers. Our technique enables a robust protocol to prepare quantum states with multiple photons in high-dimensional spaces and, as such, it constitutes a novel platform for exploring quantum phenomena in mesoscopic systems.

npj Quantum Information (2019)5:80 ; https://doi.org/10.1038/s41534-019-0195-2

INTRODUCTION

The quantum theory of optical coherence formulated by Glauber in 1963 sparked an intensive search for new states of light with exotic quantum statistics and correlations.[1–4] The possibility of reducing the quantum fluctuations of the electromagnetic field below the level of the vacuum fluctuations led to the demonstration of squeezed light in 1985.[5,6] This achievement motivated the exploration of macroscopic quantum effects using wavepackets with a large number of photons.[7] In particular, there has been an enormous interest in the generation of mesoscopic states of light that exhibit nonclassical correlations.[8,9] The generation of correlated pairs of multiphoton wavepackets has been theoretically discussed in the context of two-photon coherent states,[10] pair coherent states,[11] entangled coherent states[12] and photon-subtracted two-mode squeezed vacuum states (TMSVS).[13,14] Interestingly, over the last decades, these multiphoton states have been associated to hypothetical systems of quantum-correlated lasers.[10–12,14]

Similarly to other multiphoton states that have been employed to develop quantum photonic technologies,[15–17] it has been predicted that photon-subtracted TMSVS will play a fundamental role in applications of quantum interferometry and metrology.[14,18–20] Naturally, these ideas can also be extended and applied to the field of quantum imaging.[21] Furthermore, photon-subtracted states have been recognized as potential candidates for novel schemes in quantum information processing, quantum computing, quantum communication, and cryptography.[22–25] In addition, it has been theoretically demonstrated that photon-subtracted TMSVS are suitable to tackle intrinsic complexity problems of boson sampling and quantum photonic networks.[22] However, the engineering of photon-subtracted TMSVS remains rather elusive.[14]

Regardless of the enormous effort directed thus far at improving the efficiency of multiphoton sources,[26,27] the challenges involved in the generation and manipulation of entanglement and correlations among the photons impose practical limitations to realistic quantum technologies.[28] In 1997, Dakna and coworkers introduced the concept of photon subtraction and the possibility of performing quantum state engineering at a new fundamental level in which the quantum vacuum and the excitation mode of the fields are manipulated.[29] This work triggered a wide variety of research directions. In the context of entanglement, Takahashi et al.[30] demonstrated distillation of entanglement from a single-mode squeezed state and four years later Kurochkin and colleagues demonstrated entanglement distillation by subtracting photons from standard TMSVS.[31] More recently, Carranza and Gerry predicted the possibility of generating mesoscopic states of light with tunable average photon numbers by subtracting photons from each mode of TMSVS.[14]

Standard sources of TMSVS are based on the process of spontaneous-parametric-down-conversion (SPDC) and, under ideal conditions, they produce infinite entangled superpositions of photons as described by the expression $|z\rangle = \sqrt{1-|z|^2}\sum_{n=0}^{\infty} z^n |n\rangle_s |n\rangle_i$, where n denotes the number of photons in the signal (s) and idler (i) modes, and z represents the so-called squeezing parameter, which depends on the material properties. Typically, however, SPDC sources operate at very low brightness and the probability of generating more than one photon per mode is extremely low. This is in fact the main

[1]Quantum Photonics Lab, Department of Physics and Astronomy, Louisiana State University, Baton Rouge, LA 70803, USA. [2]National Institute of Standards and Technology, 325 Broadway, Boulder, CO 80305, USA. [3]Instituto de Ciencias Nucleares, Universidad Nacional Autónoma de México, Apartado Postal 70-543, 04510 Cd.Mx., México. [4]Max-Born-Institut, Max-Born-Straße 2A, 12489 Berlin, Germany. [5]Institut für Physik, AG Theoretische Optik Photonik, Humboldt-Universität zu Berlin, Newtonstraße 15, 12489 Berlin, Germany. *email: maganaloaiza@lsu.edu

limitation for the efficient generation of photon-subtracted TMSVS based on standard SPDC sources. Here, we circumvent this challenge by utilizing a bright SPDC source[9] in combination with photon-number-resolving detectors,[32] to demonstrate the generation of a family of correlated photon-subtracted TMSVS with a broad range of mean photon numbers and degrees of correlation. This is achieved by engineering quantum statistical fluctuations of light via conditional measurements. Our observations reveal that the generated states are composed of two multiphoton wavepackets which are highly correlated and exhibit nearly Poissonian statistics. Remarkably, this achievement constitutes an important step towards the development of entangled laser-like beams. Furthermore, this family of states inhabits high-dimensional Hilbert spaces that can be used in protocols for quantum information.[33–36]

RESULTS

Photon-subtracted TMSVS containing the same number of photons in each mode exhibit the highest degree of correlation.[14,37] Consequently, we restrict ourselves to the case of symmetric photon-subtracted TMSVS. Mathematically, the subtraction of l-photons from ideal TMSVS is obtained by applying l-times the bosonic annihilation operators $\hat{a}_{s,i}$ to the TMSVS $|z\rangle$ yielding $|z,-l\rangle = (n_s n_i)^{-1/2}|z,-l\rangle = \hat{a}_s^l \hat{a}_i^l |z\rangle = \sum_{j=l}^{\infty} B_j^{(l)} |j-l\rangle_s |j-l\rangle_i$, where $B_j^{(l)} = \mathcal{N}^{-1/2}[j!/(j-l)!]z^j$, and the normalization constant $\mathcal{N} = \sum_{j=1}^{\infty} |z|^{2j}[j!/(j-l)!]^2$. Note that by construction photon-subtracted TMSVS constitute a family of entangled states characterized by the correlation function $B_j^{(l)}$, which depends on the number of subtracted photons l and the squeezing parameter z. This implies that the degree of correlations in photon-subtracted TMSVS can be readily controlled by tuning these parameters.

For our experiments we utilize a Ti:Sapphire laser and a spectral filter, composed of two gratings and a 4f optical system, to produce 1 ps optical pulses that are used to pump a periodically poled potassium titanyl phosphate (ppKTP) waveguide with a length L of 8 mm, a nominal poling period of 46 μm and a width of 2 μm, see Fig. 1a. We produce bright TMSVS at a wavelength of 1570 nm by means of type-II parametric down-conversion process.[9] For this bright SPDC source we have the squeezing parameter given as $z = \tanh(r)$, with $r = \chi_{\text{eff}}\omega_p L\sqrt{I_p}/(2n_0 c)$, where n_0 is the refractive index and χ_{eff} is the effective nonlinearity of the waveguide, ω_p is the frequency and I_p the intensity of the pump field.

The simultaneous subtraction of l-photons is achieved by routing each of the signal and idler modes into a 90:10 fiber coupler. Each coupler subtracts photons by directing approximately 10% of the injected photons to a transition edge sensor (TES) that acts as a photon number resolving detector. The typical electrical output traces generated by a TES are shown in Fig. 1b. This information is then used to determine photon number distributions for each of the modes, see Fig. 1c. The photon events detected by the central TESs permit conditional measurements on the external TESs that register the remaining 90% of the input photons. We then monitor the correlations between the photon-subtracted states.

In Fig. 2 we present the measured joint photon number distributions (top row) for the generation of nonclassical photon-subtracted TMSVS with up to ten photons inhabiting in a multi-dimensional space for different number of subtracted photons, (a) $l = 0$, (b) $l = 1$, (c) $l = 2$, and (d) $l = 3$. It is worth noticing that the off-diagonal elements in the joint photon number distributions in Fig. 2 result from losses in the experiment. As discussed in Section S3 of the Supplementary Materials, a lossless implementation of our protocol would produce diagonal joint photon number distributions. Importantly, we observe that photon subtraction generates a family of quantum states, whose marginal photon statistics are modified from thermal to nearly Poissonian, with increasingly larger mean photon numbers, see Fig. 3. These effects become more evident for the case of $l = 3$ and $z = 0.66$, see Fig. 3d. In that particular case, we clearly observe that the marginal photon number distributions for the signal and idler modes, strongly resemble the photon number distribution that characterizes a laser (red-dashed curves in Fig. 3) with a mean photon number of $\langle n\rangle = 2.05$ and not that of a thermal distribution as in conventional SPDC sources (black-dotted curve in Fig. 3). In other words, the generated light field is composed of two wavepackets exhibiting nearly Poissonian statistics. In this sense, the generated states share some similarities with a system of entangled lasers.[14]

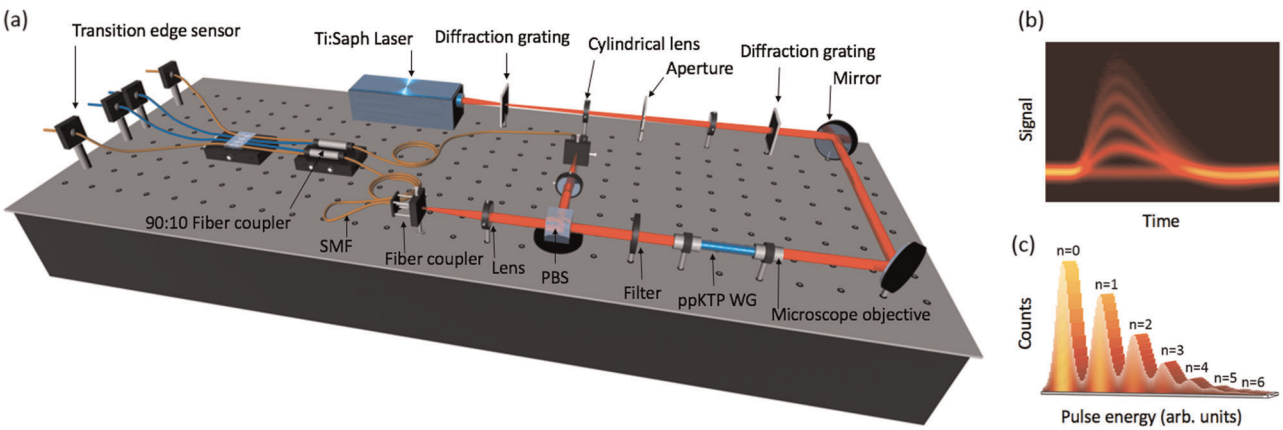

Fig. 1 A schematic representation of the experimental setup. **a** We generate two-mode squeezed vacuum states (TMSVS) through a type-II parametric down-conversion process. This is achieved by pumping a periodically poled potassium titanyl phosphate waveguide (ppKTP WG) with a femtosecond Ti:Sapphire laser at 785 nm, cavity dumped with a repetition rate of 76 MHz, which is then pulse-picked at a repetition rate of 229.166 kHz. We utilize two diffraction gratings in combination with a 4f optical system to filter the spectral profile of the pump beam. The down-converted photons are passed through a silicon filter, split by a polarizing beam splitter (PBS) and coupled into single mode fibers (SMFs). The simultaneous photon subtraction is performed on the down-converted signal and idler photons by means of two 90:10 fiber couplers that direct photons to four transition edge sensors (TESs) with photon number resolution. The electrical output traces generated by one of our TES are shown in **b**. The discrete levels of the signal demonstrate the number resolving capability of our detectors. The traces in **b** are used to obtain the pulse-energy distribution in **c**. This information is then used to determine photon number distributions for each of the modes, n represents the number of photons in a given pulse

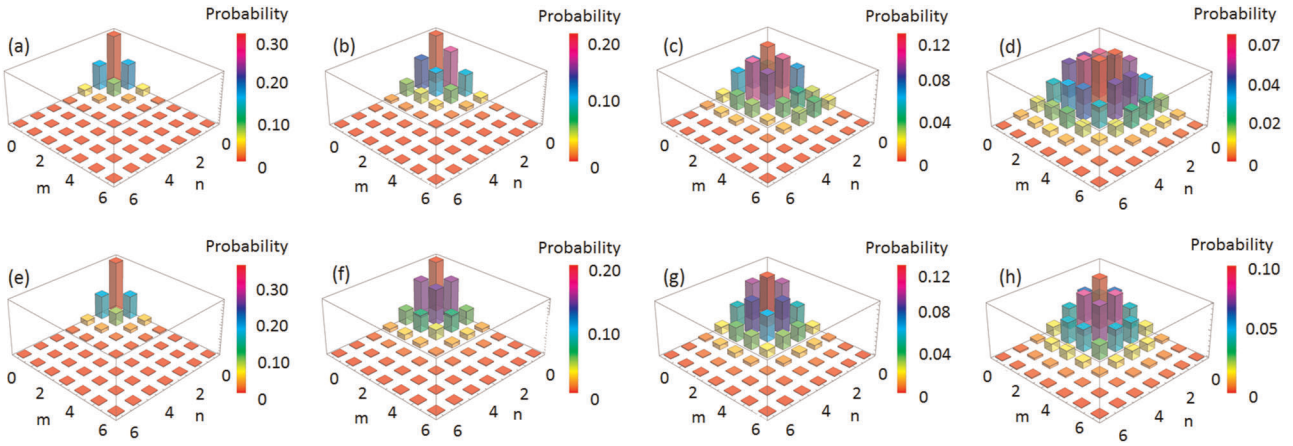

Fig. 2 Joint photon number distributions for photon-subtracted TMSVS. **a**–**d** The first row shows the experimental joint photon number distributions for the simultaneous subtraction of zero ($l = 0$), one ($l = 1$), two ($l = 2$), and three ($l = 3$) photons. **e**–**h** The bottom row shows the theoretical predictions obtained by evaluating Eq. (1)

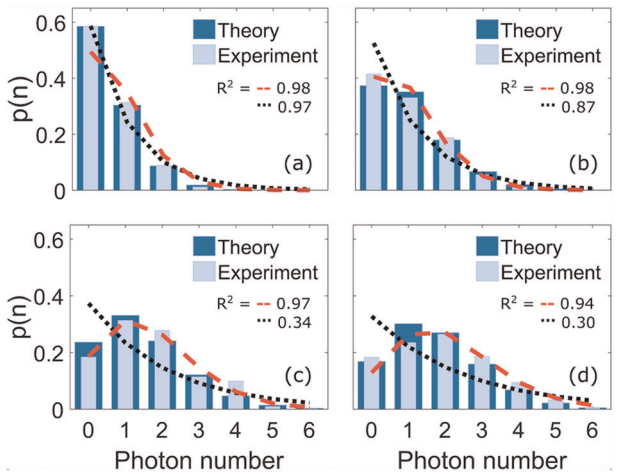

Fig. 3 Marginal photon number distributions for photon-subtracted TMSVS with l. **a** $l = 0$, **b** $l = 1$, **c** $l = 2$, and **d** $l = 3$. The overall system's efficiency is ~16.25% and the best-fit squeezing parameter is obtained to be 0.66. The red-dashed and black-dotted curves represent Poissonian and thermal photon distributions, respectively. These curves are obtained from a fit to the experimental data with mean photon numbers equal to **a** $\langle n\rangle = 0.7$, **b** $\langle n\rangle = 0.9$, c $\langle n\rangle = 1.68$, and **d** $\langle n\rangle = 2.05$. The coefficients of determination (R^2) for the fittings are shown in each panel

It is important to remark that these interesting properties of the generated multiphoton states have not been observed in previous photon-subtraction protocols.[25,30,31,38]

In order to characterize the generated states we use a theoretical model that assumes perfect TMSVS and photon detectors with non-unit detection efficiencies and contributions from dark counts. These are reasonable assumptions for sources of this kind as described in refs [9,39]. This model allows the computation of the realistic probability of simultaneously detecting m photons in the signal and n photons in the idler mode (see Section S1 of the Supplementary Materials)

$$p(n,m) = \frac{1}{n!m!}\sum_{j,k=l}^{\infty}\frac{B_j^{(l)}B_k^{(l)*}}{(j-l)!(k-l)!} \times \partial_{a}^{j-l}\partial_{a^*}^{k-l}\left\{(\eta a^* a+\nu)^n e^{-[(\eta-1)a^* a+\nu]}\right\}\Big|_{a,a^*=0} \times \partial_{\beta}^{j-l}\partial_{\beta^*}^{k-l}\left\{(\eta\beta^*\beta+\nu)^m e^{-[(\eta-1)\beta^*\beta+\nu]}\right\}\Big|_{\beta,\beta^*=0}. \quad (1)$$

Here, the parameters $\eta < 1$ and $\nu > 0$ represent the overall detector quantum efficiency, including the effect of all losses in the setup, and the dark counts, respectively.[40] Note that the complex parameters α and β arise from the Glauber-Sudarshan P-function corresponding to the photon-subtracted TMSVS.[1,41–43] It is worth remarking that the theoretical model used to obtain Eq. (1) can be readily extended to describe an asymmetric subtraction of photons from TMSVS, as well as photon subtraction from any two-mode quantum field (see Section S1 of the Supplementary Materials).

Our theoretical results, shown in Fig. 2 (bottom row) are obtained by evaluating Eq. (1), with the best fit corresponding to an overall system efficiency of 16.25%. We compare this to our estimation of the overall efficiency of our setup. The source efficiency, beam splitter transmission and detection efficiency are estimated to be 90, 90, and 80%, respectively, yielding a fiber coupling efficiency of about 25%.

The probabilistic nature of our protocol and the presence of losses reduce the possibility of successfully subtracting photons from TMSVS. In our case, we were able to subtract photons from TMSVS with the probabilities of occurrence listed in Table 1.

A natural metric to investigate the nonclassicality of the photon-subtracted states is through applying the Cauchy-Schwarz inequality $\langle(\hat{a}_s^\dagger)^2\hat{a}_s^2\rangle\langle(\hat{a}_i^\dagger)^2\hat{a}_i^2\rangle \geq |\langle\hat{a}_s^\dagger\hat{a}_s\hat{a}_i^\dagger\hat{a}_i\rangle|^2$, which is fulfilled by any classical two-mode light field. Accordingly, any violation of this inequality unequivocally indicates the nonclassical nature of any bimodal state, or equivalently that $P(\alpha,\beta)$ is nonclassical.[44] As a measure of this violation, we consider the Agarwal parameter

$$I = \frac{\sqrt{\langle(\hat{a}_s^\dagger)^2\hat{a}_s^2\rangle\langle(\hat{a}_i^\dagger)^2\hat{a}_i^2\rangle}}{\langle\hat{a}_s^\dagger\hat{a}_s\hat{a}_i^\dagger\hat{a}_i\rangle} - 1, \quad (2)$$

which is negative if the inequality is violated.[44] In Fig. 4a we present the experimental Agarwal parameter I as a function of the squeezing parameter z for the photon-subtracted states $|z, -l\rangle$ with $l = 0$, 1, 2, and 3. The theoretical curves are computed using Eq. (2) and the photon-number distributions obtained for our realistic experimental conditions through (1). For small values of squeezing ($z \to 0$) we observe the greatest degree of violation of the inequality. Conversely, by increasing the degree of squeezing ($z \to 1$) I approaches zero, i.e, a non-negative Agarwal parameter.

At this point it is worth emphasizing that not every nonclassical P-function produces a negative Agarwal parameter. Hence, we cannot rely on the Agarwal parameter to elucidate the

Table 1. Experimental probability rates of successfully subtracting *l* photons from TMSVS for various squeezing parameters *z*

z	$l=1$	$l=2$	$l=3$
0.1	6.9×10^{-5}	1.1×10^{-8}*	1.13×10^{-12}*
0.48	8.9×10^{-3}	4.5×10^{-5}	2.46×10^{-7}
0.67	1.8×10^{-3}	1.0×10^{-4}	1.39×10^{-5}

Given the low probabilities of subtracting two and three photons for states with $z=0.1$, the data with (*) indicate purely theoretical predicted values for ideal and lossless conditions

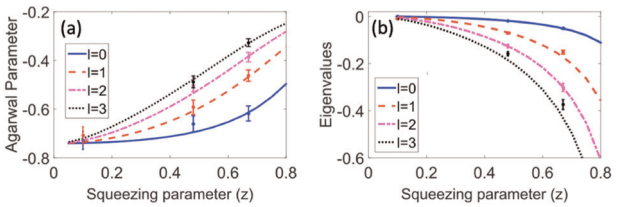

Fig. 4 Agarwal parameter and eigenvalues for the second-order matrix of moments $M^{(2,2)}$ for the generated photon-subtracted TMSVS as a function of the squeezing parameter. The Agarwal parameter in **a** certifies the nonclassical nature of *P*-function corresponding to the generated photon-subtracted states for different number of subtracted photons *l*. The eigenvalues in **b** demonstrates the possibility of tuning the degree of quantum correlations by controlling the squeezing parameter of the source and the number of subtracted photons. The curves represent our theoretical predictions for $l=0$ (blue solid line), $l=1$ (red-dashed line), $l=2$ (pink dash-dotted line), and $l=3$ (black-dotted line)

nonclassicality of the photon-subtracted TMSVS in the high squeezing regime ($z\to1$). Alternatively, to analyze the nature of the correlations between the generated photon wavepackets we explore the two-dimensional characteristic function $\sum_{m,n=0}^{\infty}p(m,n)x^m y^n$, where $p(m, n)$ is the probability of simultaneously detecting m photons in the signal and n photons in the idler modes. Then, by defining the operators $\hat{m}_{s(i)}=(\eta\hat{n}_{s(i)}+\nu)$ we obtain the joint factorial moments[45]

$$\left\langle :\hat{m}_s^u\otimes\hat{m}_i^v:\right\rangle=\sum_{m,n=0}^{\infty}p(m,n)m(m-1)\ldots(m-u+1)\times n(n-1)\ldots(n-v+1), \tag{3}$$

where : … : denotes the normal order prescription,[45] and $\left\langle :\hat{m}_s^u\otimes\hat{m}_i^v:\right\rangle$ is obtained from the *P*-function $P(\alpha,\beta)$. Using Eq. (3), it is possible to construct a matrix of moments of any order. However, it is sufficient to explore the behavior of the second order matrix of moments to demonstrate the nonclassical nature of the correlations between modes

$$M^{(2,2)}=\begin{pmatrix}\langle:\hat{m}_s^0\hat{m}_i^0:\rangle & \langle:\hat{m}_s^1\hat{m}_i^0:\rangle & \langle:\hat{m}_s^0\hat{m}_i^1:\rangle\\ \langle:\hat{m}_s^1\hat{m}_i^0:\rangle & \langle:\hat{m}_s^2\hat{m}_i^0:\rangle & \langle:\hat{m}_s^1\hat{m}_i^1:\rangle\\ \langle:\hat{m}_s^0\hat{m}_i^1:\rangle & \langle:\hat{m}_s^1\hat{m}_i^1:\rangle & \langle:\hat{m}_s^0\hat{m}_i^2:\rangle\end{pmatrix}. \tag{4}$$

Crucially, the determinant of $M^{(2,2)}$ yields information about the mean values, the variances, and the covariance of the joint-photon statistics $\det(M^{(2,2)})=\langle:(\Delta\hat{m}_s)^2:\rangle\langle:(\Delta\hat{m}_i)^2:\rangle-\langle:\Delta\hat{m}_s\Delta\hat{m}_i:\rangle^2$. For any two-mode classical field the covariance square $\langle:\Delta\hat{m}_s\Delta\hat{m}_i:\rangle^2$ is equal or larger than the product of the marginal variances $\langle:(\Delta\hat{m}_s)^2:\rangle\langle:(\Delta\hat{m}_i)^2:\rangle$ (see Section S2 of the Supplementary Materials). Thus, in order to show the nonclassicality of the correlations among the signal and idler modes, it is sufficient to show the contrary, that is, $\det(M^{(2,2)})<0$.

Table 2. Determinant of the second-order matrix of moments *M*

z	$l=0$	$l=1$	$l=2$	$l=3$
0.1	-4.06×10^{-7}	-4.82×10^{-6}	-3.05×10^{-5}*	-8.79×10^{-5}*
0.48	-0.55×10^{-3}	-6.09×10^{-3}	-19.54×10^{-3}	-15.22×10^{-3}
0.66	-6.91×10^{-3}	-62.7×10^{-3}	-202.4×10^{-3}	-332.2×10^{-3}

Notice data with (*) indicate a theoretical value predicted by Eqs. (3) and (4) using the fit values for *z*, *η*, *ν*

In Table 2, we present the experimental $\det(M^{(2,2)})$ for $l=0$, 1, 2, 3 and for three different values of *z*. Quite remarkably, as we subtract more photons, the corresponding determinant becomes more negative. This implies that by subtracting a higher number of photons the covariance square becomes much larger than the product of marginal variances, thus indicating an increasingly larger degree of correlation between modes. It is worth noticing that the determinant of $M^{(2,2)}$ produces positive values for states characterized by classical correlations such as coherent and thermal states of light. Table 2 demonstrates that different multiphoton states can be generated by selecting the squeezing parameter, defined through power of the pump beam in the source, or by subtracting different numbers of photons.

A further criterion to demonstrate the nonclassicality of the correlations is to probe the non-negativity of $M^{(2,2)}$. That is, since the matrices of moments are non-negative (positive definite) for classical states, any violation of the non-negativity implies genuine nonclassical second-order correlations for the generated photon-subtracted TMSVS (see Section S2 of the Supplementary Materials).[45] In order to demonstrate the non-negativity of *M*, we use its normalized eigenvectors $\mathbf{V}$ and the corresponding eigenvalues λ. Since $\mathbf{V}^{\dagger}M^{(2,2)}\mathbf{V}=\lambda$, if all the eigenvalues of $M^{(2,2)}$ are non-negative, it holds that $M^{(2,2)}\geq0$. On the contrary, if at least one eigenvalue is negative we have a violation of the non-negativity of $M^{(2,2)}$, that is, $M^{(2,2)}\ngeq0$. Here, we have computed the minimal eigenvalues of $M^{(2,2)}$ and the results are shown in Fig. 4b. Clearly, all the eigenvalues are negative and we can conclude that $M^{(2,2)}\ngeq0$, as a result, the correlations between the idler and signal modes are nonclassical.

DISCUSSION

It is important to notice that several metrics exist to certify nonclassicality of two-mode states.[46–48] For instance, in[46] the authors have used some uncertainty relations to establish a class of inequalities to detect entanglement. However, such a technique demands measuring expectation values of some off-diagonal operators. In the present work, however, we have opted to test nonclassicality of two-mode correlations in the sense of the Agarwal parameter.[44] Our test relies on the use of second-order moments which are directly acquired from the measured photon number distributions. This is an additional benefit of using genuine PNR detectors. Furthermore, we would like to state that, as the so-called Mandel parameter for single-mode fields,[49] the Agarwal *I* is a necessary but not sufficient condition to assert nonclassicality of the correlations among the light modes.[45,50] This can be understood from the fact that some quantum states exist for which the Agarwal parameter approaches zero and may become positive. That is, in such scenarios the non-negativity of *I* is not a sufficient condition to claim that the associated light fields are not classical. To disclose the nature of the correlations of those light fields we can always use the matrix of moments $M^{(n,n)}$.

The possibility of engineering statistical fluctuations and degree of correlation of multiphoton wavepackets complements recent demonstrations of photon-subtraction in squeezed vacuum states of light.[30,31] Indeed, the brightness of the sources and the

detection schemes utilized in the seminal experiments by Takahashi and Kurochkin enabled demonstrations of entanglement distillation. However, as discussed by Carranza and Gerry, the control of statistical fluctuations and correlations of multiphoton states via photon-subtraction is only evident at higher photon-number regimes.[14] In this regard, our work demonstrates a new degree of control of multiphoton quantum states.

Our controllable scheme for multiphoton quantum-state engineering has practical implications for multiple schemes that exploit nonclassical correlations. The role of nonclassical correlations for enhanced photodetection has been extensively studied in the context of quantum illumination.[51,52] In this regard, our protocol offers the possibility of conditioning the degree of correlation of multiphoton states to increase the robustness of quantum illumination protocols.[51,52] The post-selection of photon detection events has been exploited to overcome the fragile nature of quantum imaging protocols.[14,21] Furthermore, the control of multiphoton states at this fundamental level offers new alternatives for quantum spectroscopy. The performance of techniques for quantum spectroscopy depends on the simultaneous absorption of photons characterized by different correlation properties and mean photon numbers,[53–55] properties that can be carefully designed with our technique. Moreover, recent studies have pointed out the robustness of photon-subtracted TMSVS for quantum metrology, interestingly, the phase uncertainties for these states are less dependent on the measured phase shifts than traditional TMSVS.[14,21] Last but not least, it has been identified the enormous potential of photon-subtracted squeezed vacuum states to develop complex photonic networks with the same complexity class as boson sampling.[22] Despite the relevance of our scheme for quantum technologies, its probabilistic nature imposes important practical limitations. We believe that photonic switches and cavities can be implemented in our scheme to provide a pseudo-deterministic functionality.[56–58] This possibility will severely improve the functionality of our scheme and its potential in the development of quantum technologies.

In conclusion, we demonstrated that photon-subtracted TMSVS enables exquisite control in the engineering of multiphoton high-dimensional states. The essence of our work is given by the experimental demonstration of quantum state engineering at a new fundamental level in which the quantum electromagnetic fluctuations, mean photon numbers and degree of correlation are manipulated in a quantum state with up to ten photons. In addition, we demonstrated generation of a quantum multiphoton state, exhibiting nearly Poissonian statistics, that resembles entangled laser-like systems.[10–12,14] Our work unveils novel mechanisms to perform heralding of multiple photons, a task that remains challenging.[9] So far, it has only been demonstrated heralding of a single photon.[59] Unfortunately, the possibility of heralding multiple photons is a task of ubiquitous importance that has not been demonstrated.[9,38] In order to alleviate this limitation, the state-of-the-art in protocols for multiphoton technologies make use of multiple single-photon sources.[60–62] As demonstrated above, our technique enables the possibility of using a single source to herald two multiphoton wavepackets with specific mean photon numbers. In this case, the mean photon number of the wavepackets is predefined by the number of subtracted photons. In general, we believe that the possibility of controlling multiphoton states in high-dimensional Hilbert spaces paves the way towards new quantum protocols in the mesoscopic regime, being of particular relevance for quantum simulators,[22,28,63] quantum metrology and networks.[14,64–68]

METHODS

Detectors fabrication

The superconducting TES is a highly sensitive microcalorimeter that measures the amount of heat absorbed in the form of photons. By exploiting the sharp superconducting-to-normal resistive transition in a superconductor as an extremely sensitive thermometer, we can measure the change in resistance from absorbing one or more photons. Absorption of two photons causes a temperature rise that is ideally twice that of a single photon. As a result, the TES generates an output signal that is proportional to the cumulative energy in an absorption event. This proportional pulse-height enables the determination of the energy absorbed by the TES and consequently the direct conversion of sensor pulse-height into photon number.

We utilize Tungsten (W) as the superconductor material for the fabrication of the TESs used in this work. The device size is $20 \times 20\ \mu m^2$, with a superconducting transition temperature of ~150 mK. The W film is embedded in an optical stack designed to maximize photon absorption at the target wavelength, in this case 1550 nm. The optical stack consists of a highly reflective bottom mirror (electron-beam evaporated Ag film ~80 nm), a dielectric spacer (physical vapor deposition (PVD) grown layer of SiO2 ~232 nm thick plus a layer of direct current (DC)-sputtered amorphous-Si (a-Si) ~20 nm thick), the active detector layer (DC-sputtered high-purity W, 20 nm thick) and an anti-reflection (AR) coating (DC-sputtered a-Si ~56 nm and a PVD-grown layer of SiO2 ~183 nm). Our fiber-packaging scheme ensures sub-micron alignment of the device active area to the fiber core of SMF-28 standard telecom fiber. The optimized optical stack as well as the packaging scheme ensures detection efficiency >95% of photons transmitted through the fiber.

Detectors operation

TES are required to operate at low temperatures, below their transition temperature. Therefore, elaborate cooling systems are required to operate these devices. We operate the TESs in a commercial dilution refrigerator at a temperature around 30 mK. To operate the TESs, we voltage-bias the TESs which allows stable operation within the transition region.[69] The TES readout is typically accomplished by use of superconducting quantum interference devices (SQUIDs),[70] which serve as low noise amplifiers of the current flowing through the TES. The TES/SQUID responses due to different optical energies, i.e. photon numbers, are further amplified by room-temperature electronics and digitized. To maximize the signal to noise ratio, we perform post-processing of the output waveforms. One fast, reliable method is optimum filtering using a Wiener filter.[71] This method yields a projection of each waveform onto a known template, resulting in an outcome that is approximately proportional to the absorbed energy, hence the number of photons for a given absorption event.

DATA AVAILABILITY

The data sets generated and/or analyzed during this study are available from the corresponding author on reasonable request.

Received: 7 June 2019; Accepted: 5 September 2019;
Published online: 27 September 2019

REFERENCES

1. Glauber, R. J. The quantum theory of optical coherence. *Phys. Rev.* **130**, 2529 (1963).
2. G. S. Agarwal. *Quantum Optics Cambridge University*. (Cambridge, England, 2013).
3. Dodonov, V. V. 'Nonclassical' states in quantum optics: a 'squeezed' review of the first 75 years. *J. Opt. B* **4**, R1 (2002).
4. Scully, M. O. & Sargent, M. The concept of the photon. *Phys. Today* **25**, 38–47 (1972).
5. Slusher, R. E., Hollberg, L. W., Yurke, B., Mertz, J. C. & Valley, F. F. Observation of squeezed states generated by four-wave mixing in an optical cavity. *Phys. Rev. Lett.* **55**, 2409 (1985).
6. Loudon, R. & Knight, P. L. Squeezed light. *J. Mod. Opt.* **34**, 709–759 (1987).
7. Gerry, C. C. & Knight, P. L. Quantum superpositions and Schrödinger cat states in quantum optics. *Am. J. Phys.* **65**, 964–974 (1997).

8. Iskhakov, T. S., Chekhova, M. V., Rytikov, G. O. & Leuchs, G. Macroscopic pure state of light free of polarization noise. *Phys. Rev. Lett.* **106**, 113602 (2011).
9. Harder, G. et al. Single-mode parametric-down-conversion states with 50 photons as a source for mesoscopic quantum optics. *Phys. Rev. Lett.* **116**, 143601 (2016).
10. Yuen, H. P. Two-photon coherent states of the radiation field. *Phys. Rev. A* **13**, 2226 (1976).
11. Agarwal, G. S. Generation of pair coherent states and squeezing via the competition of four-wave mixing and amplified spontaneous emission. *Phys. Rev. Lett.* **57**, 827 (1986).
12. Sanders, B. C. Entangled coherent states. *Phys. Rev. A* **45**, 6811 (1992).
13. Kim, M. S., Park, E., Knight, P. L. & Jeong, H. Nonclassicality of a photon-subtracted Gaussian field. *Phys. Rev. A* **71**, 043805 (2005).
14. Carranza, R. & Gerry, C. C. Photon-subtracted two-mode squeezed vacuum states and applications to quantum optical interferometry. *J. Opt. Soc. Am. B* **29**, 2581 (2012).
15. Dell'Anno, F., De Siena, S. & Illuminati, F. Multiphoton quantum optics and quantum state engineering. *Phys. Rep.* **428**, 53–168 (2006).
16. Pan, J.-W. et al. Multiphoton entanglement and interferometry. *Rev. Mod. Phys.* **84**, 777 (2012).
17. Giovannetti, V., Lloyd, S. & Maccone, L. Advances in quantum metrology. *Nat. Photonics* **5**, 222 (2011).
18. Barnett, S. M., Ferenczi, G., Gilson, C. R. & Speirits, F. C. Statistics of photon-subtracted and photon-added states. *Phys. Rev. A* **98**, 013809 (2018).
19. Hofmann, H. F. Generation of a highly-phase-sensitive polarization-squeezed N-photon state by collinear parametric down-conversion and coherent photon subtraction. *Phys. Rev. A* **74**, 013808 (2006).
20. Birrittella, R. & Gerry, C. C. Quantum optical interferometry via the mixing of coherent and photon-subtracted squeezed vacuum states of light. *J. Opt. Soc. Am. B* **31**, 586–593 (2014).
21. Hashemi Rafsanjani, S. M. et al. Quantum-enhanced interferometry with weak thermal light. *Optica* **4**, 481 (2017).
22. Olson, J. P., Seshadreesan, K. P., Motes, K. R., Rohde, P. P. & Dowling, J. P. Sampling arbitrary photon-added or photon-subtracted squeezed states is in the same complexity class as boson sampling. *Phys. Rev. A* **91**, 022317 (2015).
23. Arzani, F., Ferraro, A. & Parigi, V. High-dimensional quantum encoding via photon-subtracted squeezed states. *Phys. Rev. A* **99**, 022342 (2019).
24. Huang, P., He, G., Fang, J. & Zeng, G. Performance improvement of continuous-variable quantum key distribution via photon subtraction. *Phys. Rev. A* **87**, 012317 (2013).
25. Opatrny, T., Kurizki, G. & Welsch, D.-G. Improvement on teleportation of continuous variables by photon subtraction via conditional measurement. *Phys. Rev. A* **61**, 032302 (2000).
26. Kwiat, P. G. et al. New high-intensity source of polarization-entangled photon pairs. *Phys. Rev. Lett.* **75**, 4337 (1995).
27. Eisaman, M. D., Fan, J., Migdall, A. & Polyakov, S. V. Invited review article: single-photon sources and detectors. *Rev. Sci. Instrum.* **82**, 071101 (2011).
28. Aspuru-Guzik, A. & Walther, P. Photonic quantum simulators. *Nat. Phys.* **8**, 285–291 (2012).
29. Dakna, M., Anhut, T., Opatrny, T., Knoll, L. & Welsch, D.-G. Generating Schrödinger-cat-like states by means of conditional measurements on a beam splitter. *Phys. Rev. A* **55**, 3184 (1997).
30. Takahashi, H. et al. Entanglement distillation from Gaussian input states. *Nat. Photonics* **4**, 178–181 (2010).
31. Kurochkin, Y., Prasad, A. S. & Lvovsky, A. I. Distillation of the two-mode squeezed state. *Phys. Rev. Lett.* **112**, 070402 (2014).
32. Lita, A. E., Miller, A. J. & Nam, S. W. Counting near-infrared single-photons with 95% efficiency. *Opt. Express* **16**, 3032–3040 (2008).
33. Wen, J.-M., Xu, P., Rubin, M. H. & Shih, Y.-H. Transverse correlations in tri-photon entanglement: geometrical and physical optics. *Phys. Rev. A* **76**, 023828 (2007).
34. Tillmann, M. et al. Experimental boson sampling. *Nat. Photonics* **7**, 540 (2013).
35. Perez-Leija, A. et al. Endurance of quantum coherence due to particle indistinguishability in noisy quantum networks. *Quantum Inf.* **4**, 45 (2018).
36. Kok, P. et al. Linear optical quantum computing with photonic qubits. *Rev. Mod. Phys.* **79**, 135 (2007).
37. Barnett, S. M. & Phoenix, S. J. D. Entropy as a measure of quantum optical correlation. *Phys. Rev. A* **40**, 2404 (1989).
38. Ourjoumtsev, A., Dantan, A., Tualle-Brouri, R. & Grangier, P. Increasing entanglement between Gaussian states by coherent photon subtraction. *Phys. Rev. Lett.* **98**, 030502 (2007).
39. Burenkov, I. A. et al. Full statistical mode reconstruction of a light field via a photon-number-resolved measurement. *Phys. Rev. A* **95**, 053806 (2017).
40. Sperling, J., Vogel, W. & Agarwal, G. S. True photocounting statistics of multiple on-off detectors. *Phys. Rev. A* **85**, 023820 (2012).
41. Sudarshan, E. C. G. Equivalence of semiclassical and quantum mechanical descriptions of statistical light beams. *Phys. Rev. Lett.* **10**, 277 (1963).
42. Mehta, C. L. Diagonal coherent-state representation of quantum operators. *Phys. Rev. Lett.* **18**, 752 (1967).
43. Gerry, C. & Knight, P. *Introductory Quantum Optics*. (Cambridge University Press, Cambridge, 2005).
44. Agarwal, G. S. Nonclassical statistics of fields in pair coherent states. *J. Opt. Soc. Am. B* **5**, 0740 (1988).
45. Sperling, J. et al. Uncovering quantum correlations with time-multiplexed click detection. *Phys. Rev. Lett.* **115**, 023601 (2015).
46. Hillery, M. & Zubairy, M. S. Entanglement conditions for two-mode states. *Phys. Rev. Lett.* **96**, 050503 (2006).
47. Hofmann, H. F. & Takeuchi, S. Violation of local uncertainty relations as a signature of etanglement. *Phys. Rev. A* **68**, 032103 (2003).
48. Guhne, O. Characterizing entanglement via uncertainty relations. *Phys. Rev. Lett.* **92**, 117903 (2004).
49. Mandel, L. Sub-Poissonian photon statistics in resonance fluorescence. *Opt. Lett.* **4**, 205–207 (1979).
50. Sperling, J., Vogel, W. & Agarwal, G. S. Correlation measurements with on-off detectors. *Phys. Rev. A* **88**, 043821 (2013).
51. Lloyd, Seth Enhanced sensitivity of photodetection via quantum illumination. *Science* **321**, 1463–1465 (2008).
52. Lopaeva, E. D. et al. Experimental realization of quantum illumination. *Phys. Rev. Lett.* **110**, 153603 (2013).
53. Dorfman, K. E., Schlawin, F. & Mukamel, S. Nonlinear optical signals and spectroscopy with quantum light. *Rev. Mod. Phys.* **88**, 045008 (2016).
54. Svozilik, J., Perina, J. & León-Montiel, R. de J. Virtual-state spectroscopy with frequency-tailored intense entangled beams. *J. Opt. Soc. Am. B* **35**, 460–467 (2018).
55. León-Montiel, R. de J., Svozilik, J., Torres, J. P. & U'Ren, A. B. Temperature-controlled entangled-photon absorption spectroscopy. *Phys. Rev. Lett.* **123**, 023601 (2019).
56. McCusker, K. T. & Kwiat, P. G. Efficient optical quantum state engineering. *Phys. Rev. Lett.* **103**, 163602 (2009).
57. Kaneda, F., Xu, F., Chapman, J. & Kwiat, P. G. Quantum-memory-assisted multi-photon generation for efficient quantum information processing. *Optica* **4**, 1034–1037 (2017).
58. F. Kaneda, and P. G. Kwiat, High-efficiency single-photon generation via large-scale active multiplexing. arXiv1803.04803v1 (2018).
59. Mosley, P. J. et al. Heralded generation of ultrafast single photons in pure quantum states. *Phys. Rev. Lett.* **100**, 133601 (2008).
60. Menssen, A. J. et al. Distinguishability and many-particle interference. *Phys. Rev. Lett.* **118**, 153603 (2017).
61. Spring, J. B. et al. Boson sampling on a photonic chip. *Science* **339**, 798–801 (2012).
62. Wang, H. et al. High-efficiency multiphoton boson sampling. *Nat. Photonics* **11**, 361–365 (2017).
63. Tschering, K. et al. Multiphoton discrete fractional Fourier dynamics in waveguide beam splitters. *J. Opt. Soc. Am. B* **35**, 1985–1989 (2018).
64. Ou, Z. *Multi-photon Quantum Interference*. (Springer, New York, 2007).
65. Ourjoumtsev, A., Ferreyrol, F., Tualle-Brouri, R. & Grangier, P. Preparation of non-local superpositions of quasi-classical light states. *Nat. Phys.* **5**, 189 (2009).
66. Sanders, B. C. Review of entangled coherent states. *J. Phys. A: Math. Theor.* **45**, 244002 (2012).
67. Y. Israel, et al. Entangled coherent states by mixing squeezed vacuum and coherent light, arXiv. Preprint arXiv:1707.01809v3 (2018).
68. Boto, A. N. et al. Quantum interferometric optical lithography: exploiting entanglement to beat the diffraction limit. *Phys. Rev. Lett.* **85**, 2733 (2000).
69. Irwin, K. D. An application of electrothermal feedback for high resolution cryogenic particle detection. *Appl. Phys. Lett.* **66**, 1998–2000 (1995).
70. Jaklevic, R. et al. Quantum interference effects in josephson tunneling. *Phys. Rev. Lett.* **12**, 159–160 (1964).
71. Fixsen, D. J. et al. Pulse estimation in nonlinear detectors with nonstationary noise. *Nucl. Instrum. Methods Phys. Res. A* **520**, 555–558 (2004).

ACKNOWLEDGEMENTS

We acknowledge J. P. Dowling, S. Glancy, and D. Reddy for helpful discussions. We thank N. Montaut for useful advices regarding the alignment of the waveguide

source. O.S.M-L. and C.Y. acknowledges startup funding from Lousiana State University. C. Y. acknowledges support from National Science Foundation. Contribution of NIST, an agency of the U.S. government, not subject to copyright. R.J.L.M. thankfully acknowledges financial support by CONACYT under the project CB-2016-01/284372 and by DGAPA-UNAM under the project UNAM-PAPIIT IA 100718. A.U. acknowledges support from PAPIIT (UNAM) grant IN104418, CONACYT Fronteras de la Ciencia grant 1667, and AFOSR grant FA9550-16-1-1458.

AUTHOR CONTRIBUTIONS

O.S.M-L., R.J.L-M., A.P.L, and T.G. designed the experiment. O.S.M-L. and T.G. performed the experiment. R.J.L-M, A.P.L, A.B.U., C.Y., and K. B. developed the theory. A.E.L., S.W.N. and R.P.M. fabricated the detectors, O.S.M-L, R.J.L-M., A.P-L., C. Y., and T.G. analyzed the data. O.S.M-L., R. J.L-M. and A.P.L. conceived the idea. All authors contributed to the discussion of the results and to the writing of the paper.

COMPETING INTERESTS

The authors declare no competing interests.

ADDITIONAL INFORMATION

Supplementary information is available for this paper at https://doi.org/10.1038/s41534-019-0195-2.

Correspondence and requests for materials should be addressed to O.S.M.-L.